Laser-Generated Waves and Wakes in Rotating Ion Crystals

J. M. Kriesel,[1] J. J. Bollinger,[1] T. B. Mitchell,[1,*] L. B. King,[1,†] and D. H. E. Dubin[2]

[1]*Time & Frequency Division, National Institute of Standards & Technology, Boulder, Colorado 80305*

[2]*Physics Department, University of California, San Diego, California 92093*

(Received 7 January 2002; published 7 March 2002)

Locally excited plasma waves are generated in a Coulomb crystal by "pushing" with radiation pressure on a rotating cloud of laser-cooled $^9Be^+$ ions. The waves form a stationary wake that is directly imaged through the dependence of the ion fluorescence on Doppler shifts, and theoretical calculations in a slab geometry are shown to accurately reproduce these images. The technique demonstrates a new method of exciting and studying waves in cold ion clouds.

DOI: 10.1103/PhysRevLett.88.125003 PACS numbers: 52.27.Lw, 42.50.Vk, 52.27.Jt, 52.35.–g

Clouds of trapped ions are routinely laser cooled to temperatures low enough for liquid and solidlike behavior to occur [1–4]. These so-called "Coulomb liquids" and "Coulomb crystals" offer excellent systems in which to perform basic studies of strongly coupled plasmas, soft condensed matter, and atomic physics with applications to frequency standards [5], high-precision atomic [6] and molecular spectroscopy [7,8], low-temperature chemistry [9,10], cold antimatter [11], and quantum information processing [12,13].

Previously, studies of modes of oscillation in these systems have proven extremely useful, leading to new experimental tools for probing and controlling clouds of cold charged particles [14–17]. These previous studies all utilized electric fields acting on the entire cloud to excite *global* modes. In contrast, here we excite *localized* waves by "pushing" on a cold ion cloud with the radiation pressure of a focused laser beam. In these experiments, the ions rotate relative to the push beam, and the waves interfere "downstream" to produce a stationary wake pattern, analogous to the wake behind a ship [18,19]. The technique offers a new way to locally probe and diagnose cold ion clouds and demonstrates a method for studying waves that were not accessible with previous techniques. In addition, wakes in Coulomb crystals are also a subject of current interest in their own right [20,21], due primarily to recent experiments in which Mach cones and wakes were generated in two-dimensional (2D) dusty plasma crystals [22].

Here, we use a cylindrical Penning-Malmberg trap (shown schematically in Fig. 1) to confine 15 000 to 45 000 laser-cooled beryllium ions ($^9Be^+$) at a density of $n \sim 2 \times 10^8$ cm^{-3}. The trapping fields consist of an axial magnetic field of $B = 4.465$ T and an electrostatic potential of $V_o = 1000$ V. The radius of our clouds ($R_o = 0.3$ to 2 mm) is much smaller than the radius of the trap walls ($R_w = 2.0$ cm), and the ions are confined to a small region near the trap center where the trap potential is very nearly quadratic, $\Phi_T(r, z) = m\omega_z^2(z^2 - r^2/2)/2e$ (here $\omega_z/2\pi = 800$ kHz). In such a trap, cold ion clouds are spheroidal in shape (i.e., an ellipse of revolution) described by an aspect ratio $\alpha \equiv Z_o/R_o$, where $2Z_o$ is the axial extent of the cloud at $r = 0$ and the equation $Z(r) = \pm\alpha\sqrt{R_o^2 - r^2}$ describes the boundary of the cloud [23,24].

Because of the crossed electric and magnetic fields present in the trap, the ions rotate about the trap axis at the rate ω_r. We experimentally control ω_r with a dipole "rotating-wall" perturbation [25] consisting of properly phased voltages applied to azimuthally segmented electrodes (not shown in Fig. 1). The aspect ratio of the cloud is directly related to the rotation frequency; therefore, we are able to experimentally choose a particular cloud shape by using the rotating wall to set the rotation frequency. For the data presented in this paper, $\omega_r/2\pi$ ranges from 42.5 to 128 kHz

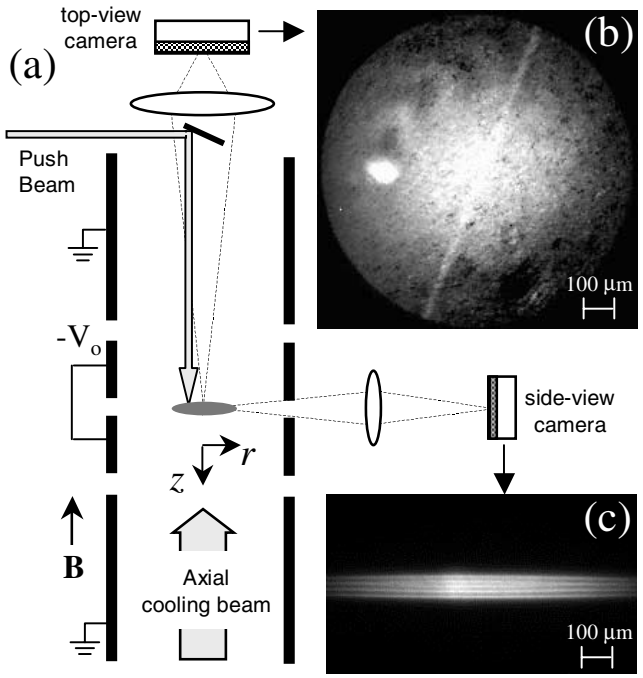

FIG. 1. (a) Schematic of the cylindrical Penning-Malmberg trap and imaging diagnostics. (b) Top-view image of the fluorescence $I(r, \theta)$ from an $\alpha = 0.042$ Be^+ ion crystal. The white spot is due to the push beam and the diagonal white line is due to a perpendicular cooling beam (not shown in the schematic). (c) Side view image of an $\alpha = 0.042$ crystal.

with a respective range in aspect ratio of $\alpha = 0.005$ (corresponding to a 2D single-plane disk of ions) to $\alpha = 1.0$ (corresponding to a 3D spherical ball of ions). For example, in Figs. 1(b) and 1(c) top and side-view images are shown for a cloud with $\alpha = 0.042$ and $\omega_r/2\pi = 45$ kHz (for both images the radial extent of the cloud $R_o \approx 860$ μm is beyond the camera's field of view).

The ions are cooled to temperatures $T \lesssim 5$ mK (giving coupling parameters of $\Gamma \gtrsim 200$) with a $\lambda = 313$ nm laser that is frequency tuned about half of a linewidth ($\sim$10 MHz) below a resonant transition in $^9Be^+$ [24]. The main (axial) cooling beam has a 500 μm waist and is directed up along the trap axis [as shown in Fig. 1(a)]; in addition, there is also a cooling beam applied perpendicular to the trap axis (not shown in the schematic). The push beam used to excite the waves is split off from the same 313 nm laser beam used for cooling, and is focused down to a relatively narrow waist $w \approx 50$ μm. As shown in Fig. 1(a), this push beam is directed antiparallel to the axial cooling beam and is offset from the rotation axis by an amount R_{pb} which we vary from 155 μm to 450 μm.

The ion fluorescence due to the axial cooling beam provides our primary diagnostic. Two sets of lenses form top and side-view images of this fluorescence on either a CCD camera or an imaging photomultiplier tube. The wakes studied here are stationary in the lab frame, allowing us to simply collect the fluorescence continuously for about 30 to 120 s to generate an image. These images provide information about coherent ion motion since the relative intensity of an ion's fluorescence is highly sensitive to its axial velocity. In essence, we have a Doppler-velocimetry diagnostic: ions moving towards the axial cooling beam (here defined to be $v_z > 0$) encounter light that is Doppler shifted closer to the resonance peak, hence they fluoresce more strongly; conversely, ions moving away from the beam ($v_z < 0$) fluoresce more weakly. For random thermal motion the variations in fluorescence average out; however, for coherent ion motion these variations enable the identification and measurement of waves and modes [17].

Figure 2(a) is an example of Doppler velocimetry for a laser-induced wake. Here we use a gray scale to show the change in fluorescence due to the laser push $\Delta I(r,\theta) \equiv I(r,\theta) - I_o(r,\theta)$; where $I_o(r,\theta)$ is a "background" image taken without the push beam, and $I(r,\theta)$ is taken with the push beam [in this case Fig. 1(b)]. The white spot in the left side of the image is due to the additional scattered light from the push beam located at a distance $R_{pb} \approx 320$ μm, whereas the downstream alternating dark and light arcs are variations in fluorescence due to coherent ion motion. We estimate that, in this case, the change in fluorescence for the first peak of the wake corresponds to a change in velocity of $\delta v_z \sim 1$ m/s [26]. We further estimate that this δv_z corresponds to a maximum displacement of $\delta z \sim 0.3$ μm [27], which is in fact much less than the interparticle spacing of $\sim$10 μm.

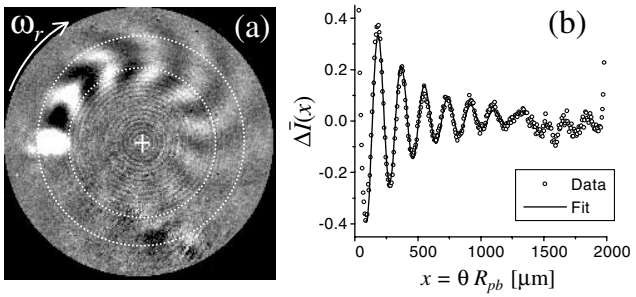

FIG. 2. (a) Differential top-view image $\Delta I(r,\theta)$ of a laser-induced wake in a clockwise rotating Be^+ ion crystal. (b) Average fractional change in fluorescence $\Delta\bar{I}(x)$ for the annular region between the white circles in (a). Here, $x = 0$ is defined to be at the center of the push beam. The solid curve is a fit to the data using a damped sinusoid [Eq. (2)].

The laser-induced wakes observed here are analogous to the wake behind a ship moving in deep water [18,19]. Because of the radiation pressure, ions receive a downward "kick" as they rotate through the push beam, similar to the kick water experiences as it passes under a moving ship. In both situations, the push excites a large spectrum of waves with different wave numbers k and frequency ω, which travel in all possible directions. Wakes that are stationary in the frame of the source occur due to the constructive interference of waves that satisfy a stationary phase condition [18,19]. The pattern of the wake depends upon the details of the appropriate dispersion relationship $\omega(k)$. The analysis of a wake is simplified directly behind the source along the direction of motion, where the stationary phase condition is satisfied by transverse [28] waves with a phase velocity ω/k that matches the relative velocity v of the source.

We thus obtain dispersion relationship data by analyzing the wakes in an annular region directly behind the push beam to obtain a wave number $k = 2\pi/\lambda$, and then use the relationship $\omega/k = \omega_r R_{pb}$ to obtain a frequency ω. For example, Fig. 2(b) is a plot of the radially averaged fractional change in intensity

$$\Delta\bar{I}(x) \equiv \frac{\int r\,dr\,\Delta I(r,x)}{\frac{1}{2\pi R_{pb}}\int dx \int r\,dr\,I_o(r,x)}, \qquad (1)$$

where the radial integrals are performed over the annular region between the circles in Fig. 2(a), and $x \equiv R_{pb}\theta$ is the rotational distance from the center of the push beam. As shown by the solid curve in Fig. 2(b), the oscillating wake is well fit by an exponentially damped sinusoid of the form

$$\Delta\bar{I}(x) = C_o + C_1 \sin(C_2 x + C_3) e^{-C_4(x/\omega_r R_{pb})}. \qquad (2)$$

Here, the C's are fit coefficients where the wave number is $k \equiv C_2$ and the damping rate is $\gamma \equiv C_4$. (In the current experiments the damping is due to the axial cooling beam.) From the fit in Fig. 2(b) we get $\lambda = 2\pi/k = 185$ μm, which in turn gives $\omega/2\pi = 490$ kHz using the calculated relative velocity of $v = \omega_r R_{pb} = 90$ m/s.

Dispersion relationship data obtained in this manner are shown in Fig. 3, where the different symbols correspond to different aspect ratios. Here the wave frequency

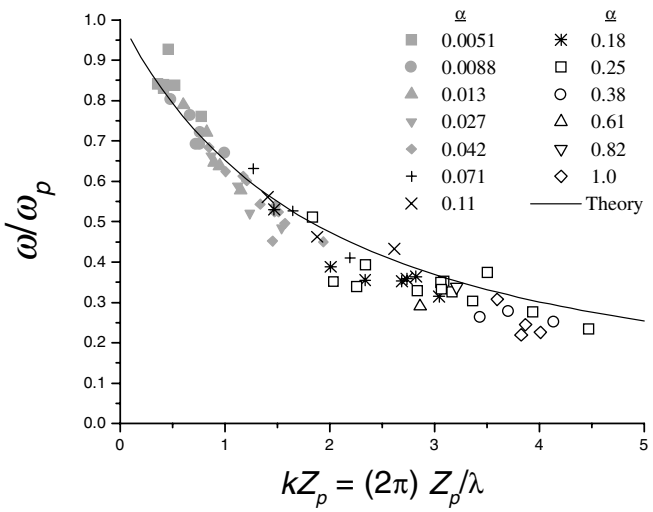

FIG. 3. Measured dispersion relationship for various aspect ratios compared to a theoretical dispersion relationship for drumhead oscillations on an infinite planar slab of cold magnetized ions with thickness $2Z_p$.

ω is scaled by the plasma frequency $\omega_p = [2\omega_r(\Omega_c - \omega_r)]^{1/2}$ [23] (where $\Omega_c/2\pi = 7.6$ MHz is the bare cyclotron frequency); and the wave number k is multiplied by half the cloud thickness at the radial position of the push beam $Z_p \equiv \alpha\sqrt{R_o^2 - R_{pb}^2}$. For a single aspect ratio, different wake patterns were generated by changing R_{pb}, which effectively changed the relative velocity v of the push beam.

To obtain a theoretical dispersion relationship, we consider fluid oscillations in an infinite, planar slab (i.e., $\alpha = 0$) consisting of a cold magnetized ion plasma. Using the cold-fluid equations [29] and the plasma dielectric constant [14], and taking the plasma thickness to be $2Z_p$, we obtain a dispersion relationship for waves with particle motion perpendicular to the plane of the slab (corresponding to axial motion in the experiments) as

$$\tan\left[\frac{kZ_p}{\sqrt{\omega_p^2/\omega^2 - 1}}\right] = \sqrt{\omega_p^2/\omega^2 - 1}\,. \tag{3}$$

For comparison to the dispersion data, we consider just the lowest-order solutions, for which the argument of the tangent ranges from 0 to $\pi/2$. The dispersion relationship for these drum-head-like oscillations is plotted as the solid curve in Fig. 3, and agrees very well with the data. While the agreement with this slab model at low-aspect ratio is better, as expected, the reasonably good agreement at higher aspect ratio ($\alpha \sim 1$) is somewhat surprising. This latter agreement indicates that the waves are excited locally and depend essentially upon the local cloud thickness, with little dependence on the global shape of the cloud.

To theoretically describe the experimental wake patterns, we account for the nonzero size of the laser beam and the rotation of the cloud and consider all solutions to Eq. (3) (not just the lowest-order solutions). Working in a frame rotating with the ion plasma, the perturbed axial velocity $\delta v_z(r, \theta, z, t)$, satisfies

$$\delta\dot{v}_z = (e/m)\partial\delta\phi/\partial z - \gamma\delta v_z + \nu\nabla^2\delta v_z + a(r, \theta - \omega_r t)\,, \tag{4}$$

where $\delta\phi(r, \theta, z, t)$ is the perturbed plasma potential, γ is again the damping rate due to the laser cooling, ν is the kinematic viscosity of the plasma, and $a(r, \theta)$ is the acceleration caused by the push beam. We model the acceleration as being proportional to the power of a Gaussian laser beam with waist w as $a(r, \theta) = A\exp(-2|\mathbf{r} - \mathbf{R}_{pb}|^2/w^2)$, where $\mathbf{R}_{pb} = (R_{pb}, \theta_{pb})$ is the location of the push beam, $\mathbf{r}$ is a position vector in the plane, and A is a scaling factor. Equation (4) is coupled to the linearized Poisson and continuity equations and the system of equations is solved in cylindrical coordinates using Fourier Bessel transforms for a plasma slab of thickness $2Z_p$. To compare to the experiments, the theoretical results are integrated in z over the plasma thickness, analagous to the integration inherent in the experimental top-view diagnostic. The resulting stationary wake pattern, as viewed in the lab frame, is written in terms of the perturbed z-averaged velocity $\langle\delta v_z\rangle$ as

$$\langle\delta v_z(r, \theta)\rangle = \frac{Aw^2}{4}\sum_{\ell=-\infty}^{\infty}\int_0^\infty k\,dk \times \frac{J_\ell(kr)J_\ell(kR_{pb})e^{i\ell(\theta-\theta_{pb})-k^2w^2/8}}{-i\ell\omega_r + \gamma + \nu k^2} \times \left[1 - \frac{\varepsilon + 1}{kZ_p}\frac{\tan(kZ_p/\sqrt{\varepsilon})}{\sqrt{\varepsilon} - \tan(kZ_p/\sqrt{\varepsilon})}\right], \tag{5}$$

where J_ℓ is a Bessel function, and $\varepsilon = -1 + \omega_p^2/[\ell\omega_r(\ell\omega_r + i\gamma + i\nu k^2)]$ is the negative of the plasma dielectric constant (including damping) evaluated at frequency $\omega = \ell\omega_r$.

In Fig. 4 experimental images $\Delta I(r, \theta)$ are shown compared to theoretical calculations. Here we use a false-color scale to represent the variations in axial velocity $\langle\delta v_z\rangle$, and scale each image by the value at the first peak of the wake. (In the experimental images, the extra fluorescence due to direct scattering of the push beam is off scale, and this region shows up as a white spot). To obtain the theory images we numerically perform the sum in Eq. (5) using experimental values for w, R_{pb}, ω_r, ω_p, Z_p, and γ. The viscosity is taken to be $\nu = 0$ since the cooling beam dominates the damping, and γ is found from the damped sinusoid fits, such as the one shown in Fig. 2(b). The image in Fig. 4(a) is the same as that shown in Fig. 2(a), where the cloud is relatively thin ($\alpha = 0.042$) with $w = 50\ \mu$m, $R_{pb} = 320\ \mu$m, $\omega_r/2\pi = 45$ kHz, $\omega_p/2\pi = 825$ kHz, $Z_p = 33.5\ \mu$m, and $\gamma = 2.3 \times 10^5\ \text{s}^{-1}$. In Fig. 4(c) we show the same cloud at a higher rotation frequency, where it is somewhat thicker ($\alpha = 0.25$); in this case, $w = 50\ \mu$m, $R_{pb} = 178\ \mu$m, $\omega_r/2\pi = 60$ kHz,

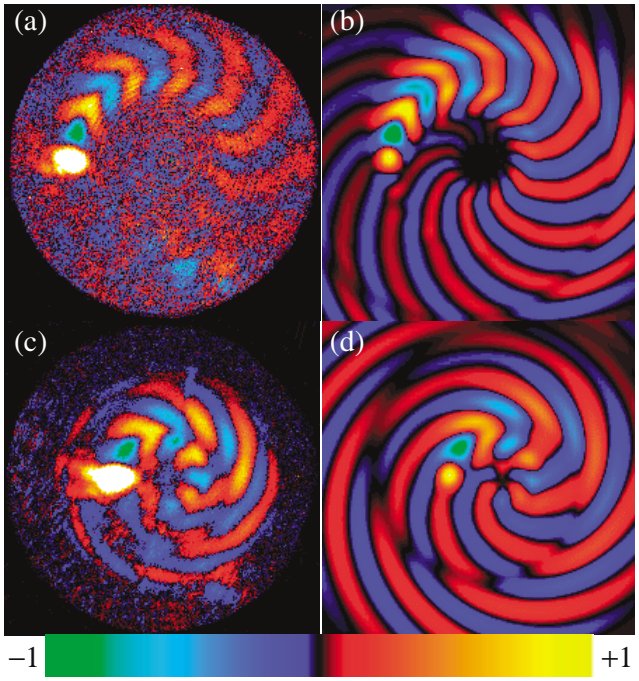

FIG. 4 (color). Scaled experimental images of wakes for clouds with (a) $\alpha = 0.042$ and (c) $\alpha = 0.25$ shown alongside corresponding theoretical calculations (b) and (d). The color scale describes relative variations in the axial velocity of the ions.

$\omega_p/2\pi = 952$ kHz, $Z_p = 98.1$ μm, and $\gamma = 1.7 \times 10^5$ s^{-1}. The theoretical calculations shown in (b) and (d), which used the above experimental values and no free parameters, are able to capture the qualitative features of the experimental images very well. For instance, both sets of images are dominated by arc-like transverse wakes; in addition, subtle features due to lateral wakes [28], such as the dark line that appears to split the transverse arcs [particularly visible in Fig. 4(d)] appear in both the theoretical and experimental images.

The experiments described here demonstrate a novel method of exciting and studying a new class of waves in cold ion clouds with potentially interesting applications. For example, the method can be used as a local probe of the cloud, providing information about such things as the local cloud thickness. In addition, with a more focused push beam than what was used here, it may be possible to excite waves with wavelengths on the order of the interparticle spacing, which should provide a probe of the ion correlations. Furthermore, with a slightly different setup, correlations may also be studied by exciting (as yet unobserved) torsional $\mathbf{E} \times \mathbf{B}$ shear modes by modulating the power of a push beam sent perpendicular to the trap axis. Such mode studies should be important for efforts to precisely control the rotational motion of the ions to a level necessary for potential applications such as quantum information processing.

This research was supported by the Office of Naval Research and the National Science Foundation (Dubin). We gratefully acknowledge Dr. M. Jensen and Dr. B. Jelenković for useful comments on this manuscript.

*Current address: Department of Physics and Astronomy, University of Delaware, Newark, DE 19716.
†Current address: Department of Mechanical Engineering, Michigan Technological University, Houghton, MI 49931.

[1] H. Walther, Phys. Scr. **T59**, 360 (1995).
[2] W. M. Itano *et al.,* Science **279**, 686 (1998); T. B. Mitchell *et al.,* Science **282**, 1290 (1998).
[3] L. Gruber *et al.,* Phys. Rev. Lett. **86**, 636 (2001).
[4] L. Hornekær, N. Kjærgaard, A. M. Thommesen, and M. Drewsen, Phys. Rev. Lett. **86**, 1994 (2001).
[5] J. N. Tan, J. J. Bollinger, and D. J. Wineland, IEEE Trans. Instrum. Meas. **44**, 144 (1995).
[6] J. J. Bollinger *et al.,* Phys. Rev. Lett. **63**, 1031 (1989).
[7] T. Baba and I. Waki, Jpn. J. Appl. Phys. **35**, L1134 (1996).
[8] M. A. van Eijkelenborg, M. E. M. Storkey, D. M. Segal, and R. C. Thompson, Phys. Rev. A **60**, 3903 (1999).
[9] K. Mølhave and M. Drewsen, Phys. Rev. A **62**, 011401(R) (2000).
[10] G. H. Dunn, Phys. Scr. **T59**, 249 (1995).
[11] B. M. Jelenković *et al.,* in *New Directions in Antimatter Chemistry and Physics,* edited by C. M. Surko and F. Gianturco (Kluwer Academic, The Nederlands, 2001), Chap. 1.
[12] J. I. Cirac and P. Zoller, Phys. Rev. Lett. **74**, 4091 (1995).
[13] D. J. Wineland *et al.,* J. Res. Natl. Inst. Stand. Technol. **103**, 259 (1998).
[14] D. H. E. Dubin, Phys. Rev. Lett. **66**, 2076 (1991).
[15] M. D. Tinkle *et al.,* Phys. Rev. Lett. **72**, 352 (1994).
[16] J. J. Bollinger *et al.,* Phys. Rev. A **48**, 525 (1993).
[17] T. B. Mitchell, J. J. Bollinger, X.-P. Huang, and W. M. Itano, Opt. Express **2**, 314 (1998).
[18] Lord Kelvin (Sir W. Thomson), Proc. R. Soc. of London **42**, 80 (1887).
[19] T. E. Faber, *Fluid Dynamics for Physicists* (Cambridge University Press, Cambridge, United Kingdom, 1995).
[20] D. H. E. Dubin, Phys. Plasmas **7**, 3895 (2000).
[21] X. Wang, A. Bhattacharjee, and S. Hu, Phys. Rev. Lett. **86**, 2569 (2001).
[22] D. Samsonov *et al.,* Phys. Rev. Lett. **83**, 3649 (1999); D. Samsonov *et al.,* Phys. Rev. E **61**, 5557 (2000); A. Melzer *et al.,* Phys. Rev. E **62**, 4162 (2000).
[23] D. H. E. Dubin and T. M. O'Neil, Rev. Mod. Phys. **71**, 87 (1999).
[24] L. R. Brewer *et al.,* Phys. Rev. A **38**, 859 (1988).
[25] X.-P. Huang, J. J. Bollinger, T. B. Mitchell, and W. M. Itano, Phys. Rev. Lett. **80**, 73 (1998).
[26] Here we use the slope of the resonant transition curve at a detuning of 10 MHz.
[27] Here we use $\Delta z = \Delta v_z/\omega$ with $\omega/2\pi = 490$ kHz, where the method for obtaining this value of ω is described later in the text.
[28] In this context "transverse" means that the wave fronts are approximately perpendicular to the direction of motion, in contrast to "lateral" where the wave fronts are approximately parallel to the direction of motion.
[29] A. W. Trivelpiece and R. W. Gould, J. Appl. Phys. **30**, 1784 (1959).